Original Article

Modeling and Simulation of Piezo-beam Structure Mounted in a Circular Pipe using Laminar Flow as Energy Harvester

Mohit Yadav[1], Surendra Kumar[1], Ashish Kaushik[2], Ramesh Kumar Garg[2], Akash Ahlawat[3],
Deepak Chhabra[3*]

[1]Department of Applied Sciences, University Institute of Engineering and Technology, M D.U Rohtak, Haryana, India.
[2]Department of Mechanical Engineering, DCRUST, Murthal, Sonipat Haryana, India.
[3]Department of Mechanical Engineering, University Institute of Engineering and Technology, M. D.U Rohtak, Haryana, India

[*]Corresponding Author: deepak.chhabra@mdurohtak.ac.in

Abstract - *With the advancement in nanotechnology and wireless electronic devices, it has become necessary to build an utterly self-powered device that relies on micro-power sources. Due to adverse and complicated conditions of the environment in the sea, supplying energy and voltage to ships, submarines, and other sea equipment has become a very tough task. So, green energy harvesting system has made remarkable progress in this field. Keeping this in view, there is a scope to develop an effective, efficient and stable model for piezoelectric energy harvesting that can withstand the high pressure of flowing water. The main vision of the present system is to offer a renewable source of energy that may not only produce continuous energy from waste flowing water and available energy of surroundings but can be used as a feasible solution to power portable electronic devices. Therefore, in the current proposed work, an effort has been made to design the proposed setup of the piezoelectric energy harvesting structure with hydro-dynamism via mathematical modelling and simulation. Modelling and simulation have been done by ANSYS software by the striking of laminar flowing water with a mean velocity of '30 m/s' on a circular cylindrical structure of length '1000 mm' with diameter '200 mm', containing a rectangular beam and PZT piezoelectric plate at a distance of '202.698 mm' from an inlet of the cylinder. The phenomena of vortex shedding occurred behind the bluff body by striking flowing fluid. Consequently, the piezoelectric beam structure started to oscillate. As a result of this vibration, a voltage of 0.026V has been generated within the beam and piezoelectric patch arrangement, and it can be stored in batteries for future purposes.*

***Keywords** - Renewable energy harvesting, Fluid-structure interaction, Simulation, Mathematical modeling, Computational fluid dynamics (CFD), Voltage generation.*

1. Introduction

The 21st century is an era of industrial and technological revolution, and there is a massive requirement for self-power sources for moveable gadgets and wireless setup of networking models [1]. With the substantial rise in demand for electricity and equally huge concern about carbon emission, clean energy, and the global warming issues created by the consumption of fossil fuels resulting in pollution created by chimneys of coals and fired power plants. The pollution created by the chimneys of coal hits many health hazardous problems for the public. Six power plants remain inoperative in Delhi from 16th November to 30th November 2020 to improve air quality in India's Commission for Air Quality Management (CQAM) [2]. As a result, the whole world has been shifting toward renewable clean energy harvesting sources [3-6]. In this modern area of renewable energy harvesting, such as piezoelectric energy harvesting, has

noticed a critical improvement in the past few decades [7-8]. Consequently, investment in piezoelectric energy harvesting has been hiked from $145 million to $667 million from 2018 to 2022[9]. This growth evidently shows the importance of renewable energy harvesting with piezoelectric materials from the previous century. The increasing demand for renewable green energy harvesting in the current scenario is due to its environmental-friendly behaviour, ease of coping with other systems, inexpensive and smoothly accessible in the environment [10].

Harvesting energy from piezoelectric materials plays a significant role in this direction of their capability to transform a mechanical vibrational form of energy into an electrical form of energy [11]. Due to the downfall in electricity of frequently applicable devices, researchers are concentrating on innovating smart circuits, models, and grid techniques that can

yield energy from mechanical devices and transfer electricity to moveable electronic gadgets [12]. Piezoelectric materials can generate electric power from stress and vibrations induced by flowing fluid. When the fluctuating force of flowing fluid strikes a piezoelectric material, it generates electricity [13-14]. The generated energy can be preserved in storage systems for various purposes. The source of flowing fluid can be wastes of factories, power plants, industries, and households which can be freely available in the environment for generating electricity at a micro level [15-16].

The power can be generated from the micro-watt range to mega-watt depending on various factors like the velocity of flowing fluid, the pressure of striking on the piezoelectric patch, properties of the piezo-patch, arrangement of the circuit, orientation of the fluid-structure body and distance of patches from flowing fluid, number of patches and dimension of patches [60-65]. Hydro-mechanical power of piezoelectric materials has a wide range of applications [67]. This technique helps utilize the pressure of flowing fluid and convert it to usable electric energy for portable electronic devices [18]. Harvesting of energy using hydro dynamism can be used to fabricate a computerized submerge machine for supplying regular electrical energy for underwater imaging. Such energy harvesters can be applicable to mimic biomimetic movements like an eel and fish motion. Blood flowing in human arteries and veins is also a feasible type of fluid streaming source for nano-scale devices that can act as a bio-sensor. Nano pumps and nanogenerators are designed to generate hydroelectricity using piezo materials that can be used to power NEM devices [19]. The concept of hydroelectricity generation with piezoelectric materials is quite feasible to remove the extra burden and dependence on non-renewable energy harvesting sources. In the surroundings, there are large numbers of water

bodies like rivers, canals, waste sewages, etc. which have flowing water having kinetic energy. This waste kinetic energy produces vibrations [20].

Piezoelectric materials can easily convert these vibrations into electrical energy [21-22]. Since the batteries have the disadvantage of having a finite lifespan, the piezoelectric material may be the ideal solution. [23]. Thus, the PEHF system can be the best energy source for powering MEMs and NEMs as it can easily convert fluid vibrations into valuable electric energy[68]. Yadav et al. have done the modeling and simulation of piezoelectric green energy harvesting for an open channel flowing fluid by considering various parameters like the flowing rate of fluid, configurations of circuits, turbulency, location of piezoelectric patches, and film[25-28]. Different optimization techniques have been developed from time to time for the solution of non-linear numerical models [54-57]. Yadav et al. have done the simulation of a turbulent flowing model with a finite element analysis technique for piezoelectric energy harvesting [58,59]. An initial literature review has been done, covering all the bases for energy harvesting using mechanical vibrations. [29-30].

The interaction of several categories of piezoelectric materials and mechanical vibrations has been used to examine numerous aspects of energy harvesting, as shown in Figure 1. Using different piezoelectric materials, many researchers developed models to analyze and compare the efficiency of PEH devices[31]. To investigate the direct and converse piezoelectric effect, many micropower generators designed using different piezoelectric structures have been discussed[32].
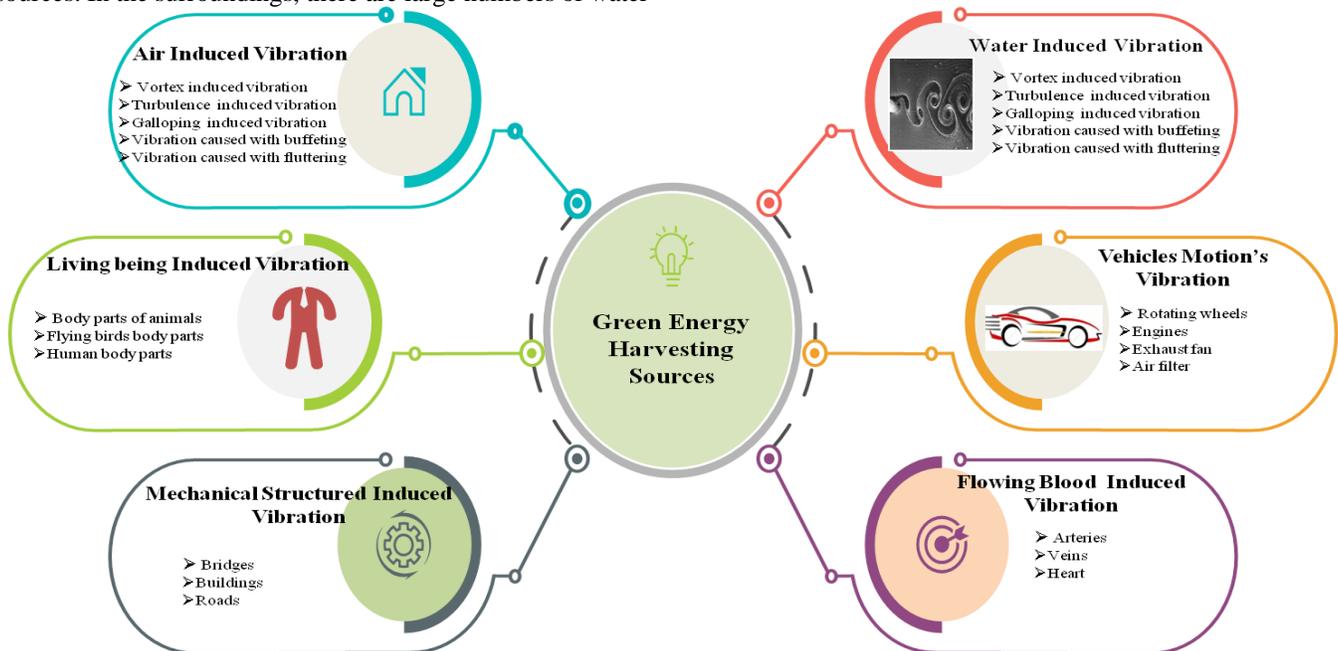

Fig. 1 Sources of energy harvesting with interaction of piezoelectric smart materials

Furthermore, a review of many aspects of energy harvesting from sources like electric/magnetic field sources and human body movements using various piezoelectric materials has been given by Panda et al. [66]. Hu et al. have been harvested piezoelectricity from different fluid sources like vortex flow(V.F.), river, ocean waves, close channel flow, open channel flow, flutters, and freely falling drops using different structural configurations like cantilever beam, plate, film, shell, ring, patch, circular diaphragm [34-38]. With the growing field in energy harvesting and their storage medium, many researchers have looked upon the ability to extract the maximum amount of energy from piezoelectric materials[39-41].

Various research has been done by scientists on numerical modeling and optimization of piezoelectric renewable energy harvesting sources by considering the various parameters such as the various arrangement of fluid structures, the configuration of circuit patches in series and parallel, the velocity of flowing fluid with various distances and angles, the amplitude of striking sea wave on piezo-patches[42-45]. Various sources of green energy harvesting sources can be seen in fig. 1.

The work done to design and optimize voltage, power, and energy with different structural configurations to obtain maximum benefits from the harvesting system has been investigated [46-47]. Many researchers use different circuit configurations or develop piezoelectric actuators and circuits to obtain maximum benefits from the harvesting system [48-52]. The main part of previous research is focused on modeling the cylinder and simulation results. For the small size right circular cylinder, the phenomenon of wake oscillation of striking fluid has happened, while for large size cylinder, the vibration induced by vortex flow has been

accurately predicted by researchers for simulation and modeling purposes. Since the development of hybrid systems has received much less attention than other energy harvesting systems, so, it is necessary to design an efficient, feasible and stable model which can bear the impact of flowing water for various configurations of piezo patches, circuits and harvest energy in the most feasible way.

A good mathematical model has been designed such that it can be easy to understand, and all the included parameters in modeling have some physical interpretation with a wide variety of applications. Due to mathematical modeling, the phenomenon can be easy to understand for prediction and software results. The model guarantees the validity and reliability of the phenomenon and has various scopes for growth in the future.

2. Construction and Operating Mechanism of Model

The current proposed model is composed of a circular cylinder with an outer diameter of '200 mm', an inner diameter of 180 mm', a thickness of '10 mm' and a length of cylinder' 1000 mm'. A beam with the dimension 47.973x20x20 mm' and rectangular piezoelectric smart material PZT 5A having dimension 37.973x20x20 mm' has been attached inside it with a distance of 202.698 mm from an inlet of the circular cylinder as demonstrated in fig. 2.

The primary aim of the current setup is to change the kinetic energy (K.E) of flowing water with an average velocity 'of 30 m/s into electrical energy via piezoelectric smart material. The overall configuration and dimensions of the model which have used in this proposed work are listed in Table 1.
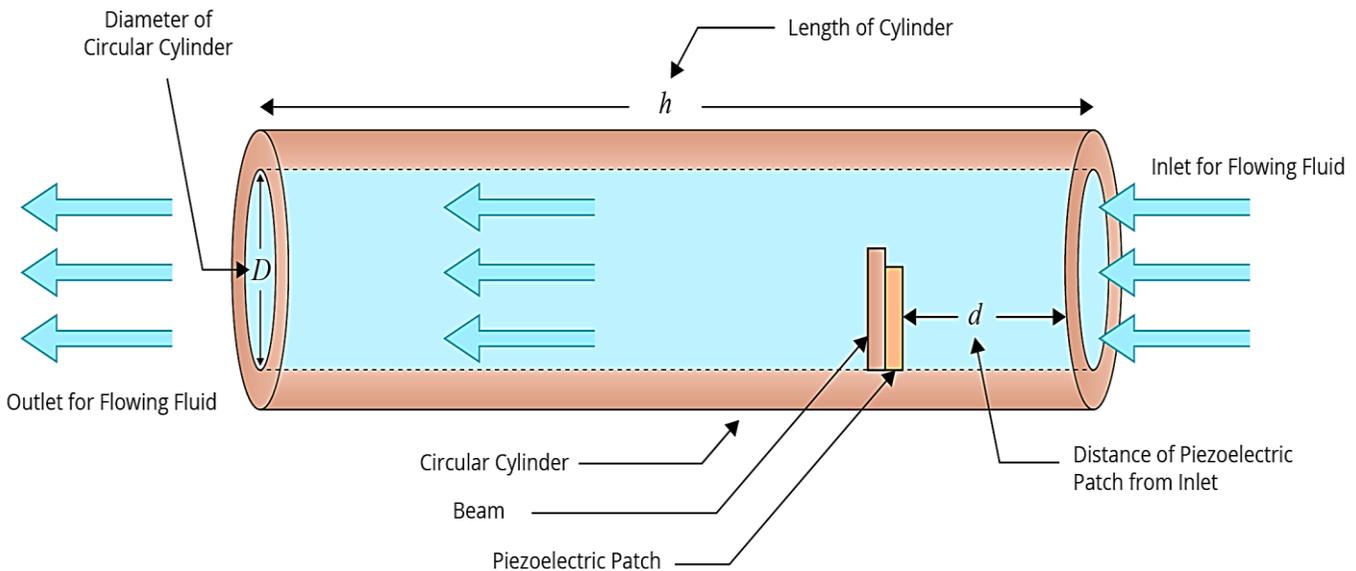

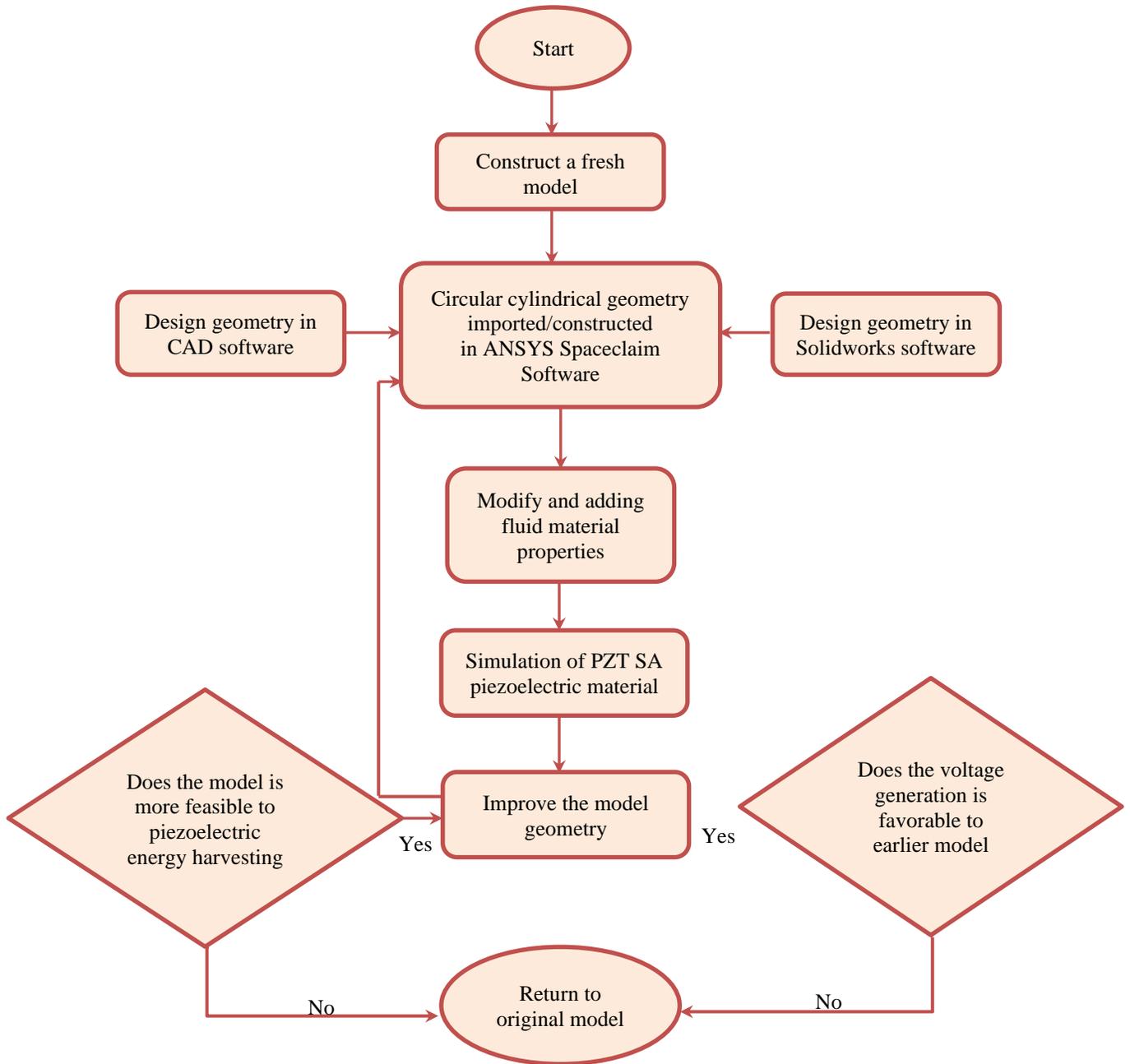**Fig. 2 Flow-based piezoelectric energy harvester as a 3- dimensional geometry**

Fig. 3 Workflow of piezoelectric energy harvester through simulation

3. Modeling and Simulation of Fluid-Structure Interaction in ANSYS

The modeling and simulation of various engineering challenges can be accomplished effectively with the help of the ANSYS software. In the current proposed setup, an effort has been made to design the piezoelectric green energy harvesting structure's feasible model using hydro-dynamism via mathematical modeling. The model has been simulated using ANSYS software to assess different mechanical analyses of the small-scale energy harvesting model, such as the physical state of strain and stress in the circular cylindrical systems. The finite element analysis (FEA) technique is used. Stationary analysis has been used to express the practicability of the proposed model. The combination of a rectangular piezoelectric patch of type PZT 5A and a beam mechanism has been attached to the circular cylinder. A step-by-step explanation of the modeling process, as well as the simulation results of the mechanical structure, is provided and can be seen in fig. 3. The findings provide validity to the hypothesis that the MEMS energy harvester will be based on fluid flow. The following section demonstrates the stages involved in modeling and simulating a circular cylinder piezoelectric energy harvester using ANSYS software.

Table 1. Parameters with their dimensions of the proposed energy harvester

| Parameters	Description	Values	Unit	Parameters	Description	Values	Unit
D_0	Outer Diameter of Circular Cylinder	0.20	m	D_i	Inner Diameter of Circular Cylinder	0.18	m
T_c	Thickness of Cylinder	0.01	m	L_c	Length of Cylinder	1	m
ρ_{ss}	Density of Structure Steel	7850	kg/m³	l_B	Length of Embedded Beam	0.047	m
W_B	Width of Embedded Beam	0.02	m	T_B	Thickness of Embedded Beam	0.02	m
L_{PZT}	Length of PZT 5A Piezo-patch	0.037	m	B_{PZT}	Breadth of PZT 5A Piezo-patch	0.02	m
h_{PZT}	Thickness of PZT 5A Piezo-patch	0.02	m	u	Inlet Flow Velocity	30	m/s
ρ_w	Density of Fluid	997.77	kg/m³	ρ_{st}	The density of the Structure Steel	7850	kg/m³
η	Viscosity of Fluid	0.001	Kg/ms	ν	Kinematic Viscosity	1	mm^2/s
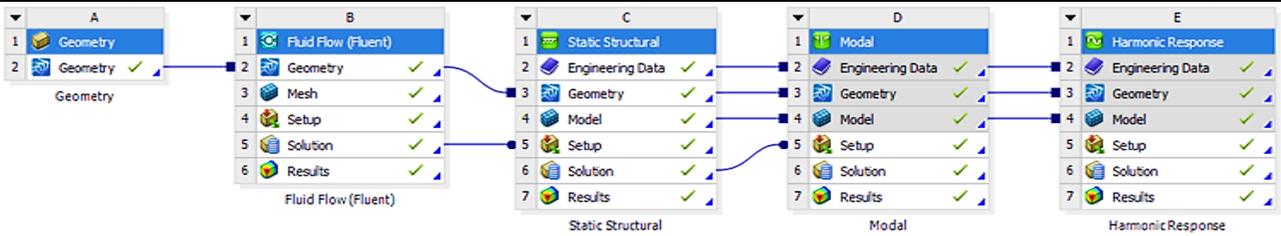
Fig. 4 Classic workflow for simulating fluid-structure interaction with ANSYS

3.1. Developing Geometry in ANSYS

The device's geometry is an essential design issue that must be taken into account. Because of the space limitations imposed by the application, the geometry needs to be optimized to have a low natural frequency while preserving a high power density. The device geometry can be seen in figure 2, and it comprises a circular cylinder attached material with a rectangular piezoelectric patch PZT 5A and beam inside it. The geometrical and mechanical characteristics of the device are detailed in table 1.

3.2. Addition of Materials in Model

In the simulations, circular cylinders and beams were assigned with structural steel as material. The piezo-smart material employed as Lead Zirconate Titanate (PZT 5A), the material used for fluid flow, has been assigned as water.

3.3. Addition of Physics in Simulation

The rectangular piezoelectric devices physics are added to the study, which consists of fluent, static structure, and solid mechanics with the harmonic response as an additional study area can be seen in fig. 4. Maximum displacements, strains, and stress are some of the findings of solid mechanical physics. Through the use of a static structural, electric field, electric potential distribution, frequency response, phase response, and output voltage can be analyzed. Setting the boundary conditions means fixing the bottom faces of the beam and piezoelectric patch, which are attached to a circular cylinder while letting all the other domains move around freely. Linear elastic characteristics such as young modulus, density, Poisson ratio, Anisotropic dielectric permittivity matrix, Anisotropic elastic stiffness polarization matrix, and piezoelectric stress matrix with electric field vector can be selected from the library of ANSYS engineering data, and their values retrieved automatically.

The velocity of the flowing fluid for the inlet wall is taken as 30 m/s while the pressure value for outlet backflow is set to zero. The top of the piezoelectric layer is given a floating potential. The various used matrices in fluid-structure interaction (FSI) are as follows:

1. Anisotropic elastic stiffness polarization matrix in the y direction is

$$\begin{bmatrix} 1.20E+11 & 7.52E+10 & 7.51E+10 & 0 & 0 & 0 \\ 7.52E+10 & 1.20E+11 & 7.51E+10 & 0 & 0 & 0 \\ 7.51E+10 & 7.51E+10 & 1.11E+11 & 0 & 0 & 0 \\ 0 & 0 & 0 & 2.26E+10 & 0 & 0 \\ 0 & 0 & 0 & 0 & 2.11E+10 & 0 \\ 0 & 0 & 0 & 0 & 0 & 2.11E+10 \end{bmatrix}$$

2. Anisotropic Dielectric Permittivity at constant mechanical strain matrix in the y direction is

$$\begin{bmatrix} 1.99E-09 & 0 & 0 \\ 0 & 1.99E-09 & 0 \\ 0 & 0 & 5.78E-10 \end{bmatrix}$$

3. Matrix for Piezoelectric stress with an electric field vector is

$$\begin{bmatrix} 0 & 0 & 5.35116 \\ 0 & 0 & 5.35116 \\ 0 & 0 & 15.78347 \\ 0 & 0 & 0 \\ 0 & 12.29474 & 0 \\ 12.29474 & 0 & 0 \end{bmatrix}$$

3.4. Modification of the Model and Implementation in ANSYS

The cylinder is assumed to be stiff in three-dimensional simulations (as seen in fig. 2). Five distinct interfaces have been used in the simulation.

1. Viscous flow: to simulate the flow pattern by modeling
2. Meshing: to model the deformation that occurs in the fluid domain.
3. Static Structural: for simulating the piezoelectric solid domain structures and to model the charge conservation in piezoelectric materials.

4. Electric Circuit: to simulate the workings of the harvester circuit.
5. Harmonic Response: For the purpose of simulating the phenomena like stress-strain, phase response, frequency response, and voltage frequency phenomena.

Two different mechanical interfaces are incorporated into the model.
1. Piezoelectric Effect: for the purpose of linking the fields of Static-Structural and Solid Mechanics.
2. Fluid-Structure Interaction (FSI): to couple Solid Mechanics and laminar flow model.

3.5. Creation of Meshing

The ANSYS software comes with various meshing options that can be used at any level with any method and element size. Fluent uses the face selection command to specify the solid-fluid interface as well as the inlet and outlet for meshing. In this investigation, the triangular mesh was employed with an element size of 0.00025 m. A total of 220218 domain elements have been found to constitute a full mesh as a result of the meshing process. The meshing has been calibrated by general physics with a predefined normal type size. The maximum element expansion rate of 1.2 has smooth transition inflation with a ratio of 0.272 and pinch tolerance of 0.00046 m.
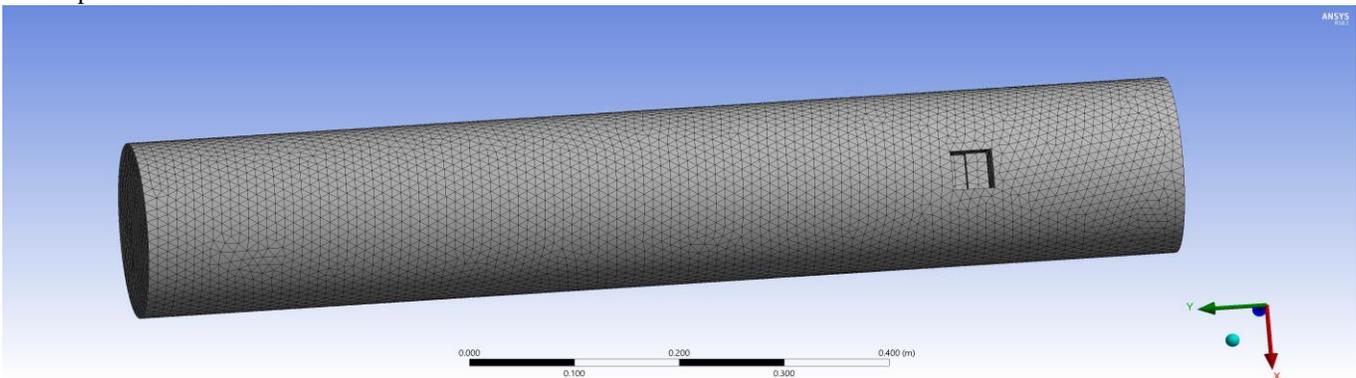

Fig. 5 Free triangular meshing structure of the circular cylindrical structure
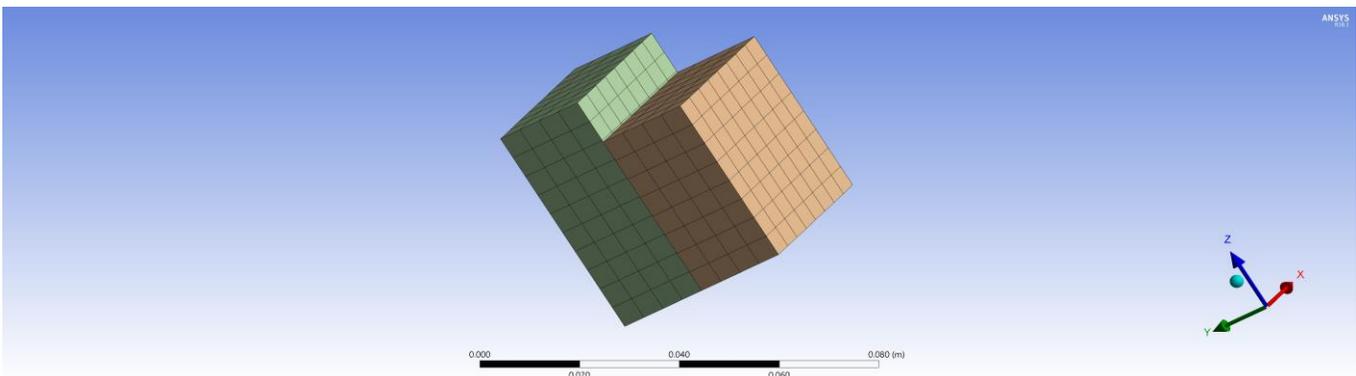

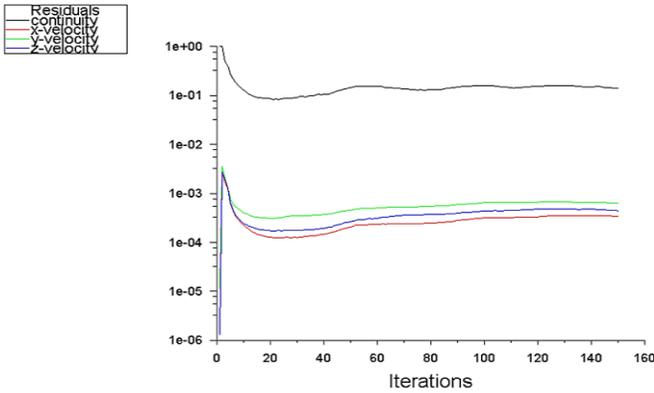**Fig. 6 The meshing of beam-piezoelectric patch structure**

Fig. 7 Residual graph for velocity vs no. of iterations

Figure 5 depicts the final mesh geometry that was generated. Meshing has been done by software with 150 iterations in residual form with different velocity components in the x,y, and z directions. The graph of velocity residuals vs no. of iterations can be shown in fig. 7.

In the case of a rectangular piezoelectric patch and beam, a total of 448 domain elements and 2566 nodes were found to constitute a full mesh as a result of the meshing process, as shown in fig 6. The meshing has been calibrated by general physics with a predefined normal type size. The element size of 0.005 m parameters has been taken maximum element expansion rate of 1.2, having a smooth inflation transition ratio of 0.272, pinch tolerance of 0.0059 m, and minimum and maximum face size is 0.00656 m to 0.032 m, respectively.

3.6. Selection of Structural Components and Body Sizing in ANSYS
3.6.1. inlet
The inlet for the flowing fluid of the circular cylinder can be shown in fig. 8 by selecting the red portion as the face of the cylinder in the y direction.

3.6.2. Outlet
The outlet for the flowing fluid of the circular cylinder

can be shown in fig. 9 by selecting the red portion as the face of the cylinder.

3.6.3. Wall
The wall for the flowing fluid of the circular cylinder can be shown in fig. 10 by selecting the red portion of the cylinder.

3.6.4. Fluid Solid Interaction(FSI)
The interaction of flowing fluid with a solid structure of a circular cylinder can be shown in fig. 11 by selecting the red portion of the cylinder.

3.7. Post-Processing CFD Simulation and Static Structural Analysis
This research aims to analyze the consequence of varying the factors on the voltage generation capacity of a piezoelectric energy harvester with a circular cylinder and beam arrangement. All the equations and analysis of models have been solved mathematically in three dimensions using the finite element technique with the ANSYS software. In addition, during preprocessing, the boundary conditions for the piezo-patch, such as fluid-solid interface, fixed support, and preliminary operational setting, are approached in the analytical environment. This is done to obtain the constants for the mathematical solution produced using the finite element technique. Moreover, the viscous laminar fluid is simulated with water as the flowing material (fluent). This modeling is performed in collaboration with the boundary conditions. The setup's initialization, an average velocity of 30 m/s at the inlet, while fluid pressure has been imported at the piezoelectric plate and outlet. As the flowing fluid strikes on piezoelectric material with an average velocity of '30m/s', then the velocity and pressure contour plots can be observed by assuming the yz plane as a working coordinate system in fig. 12 & 13, respectively. At the peak of inflow velocity as '37.720 m/s', the ANSYS simulation produced the following pressure contour with the maximum pressure value of 590.1002 [Pa].
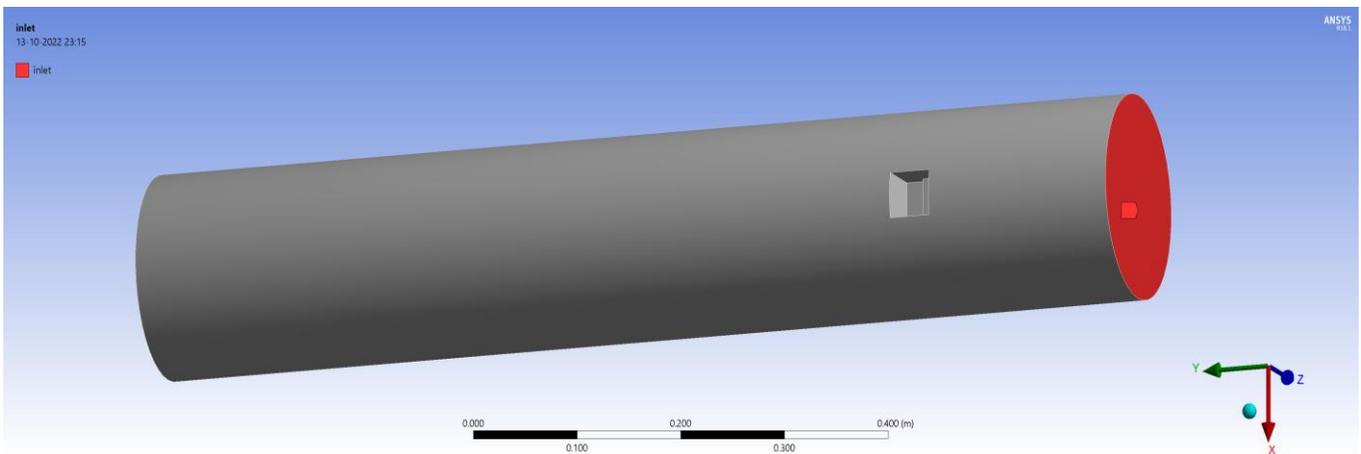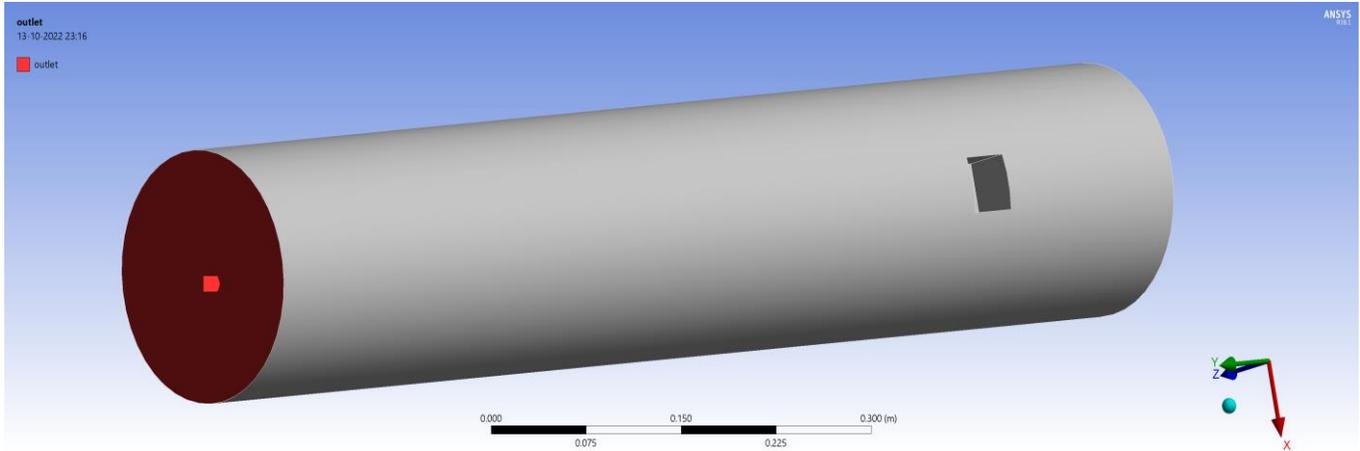

Fig. 8 Inlet of the cylindrical structure

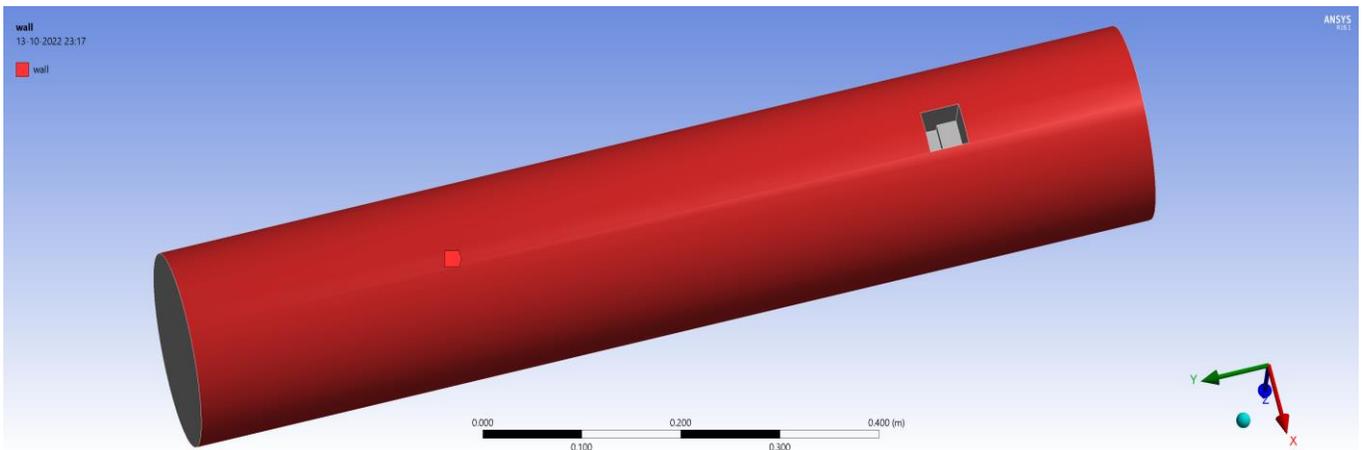**Fig. 9 Outlet of the cylindrical structure**

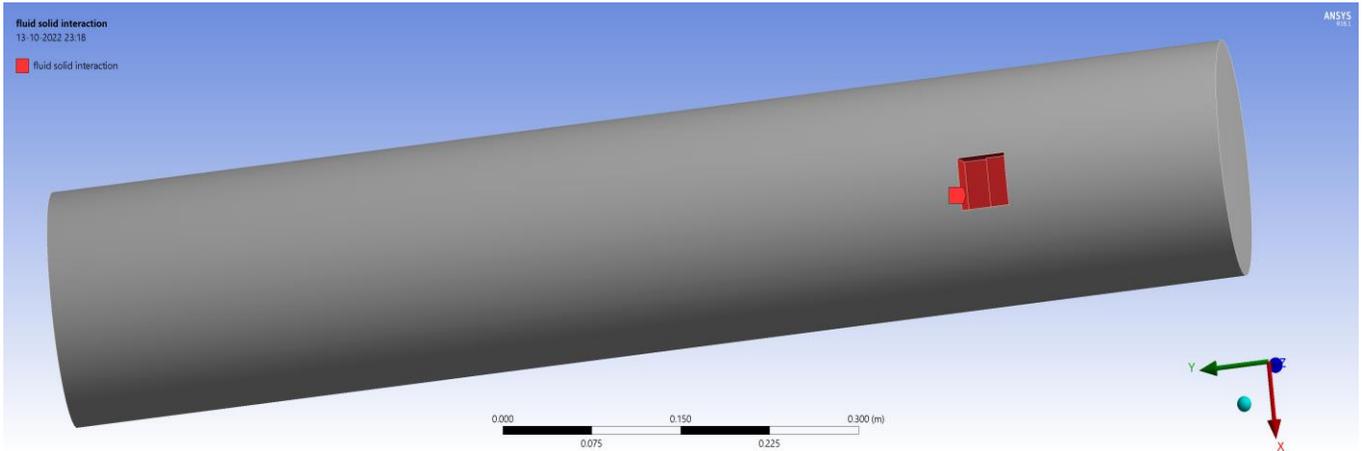**Fig. 10 Wall of the cylindrical structure**

Fig. 11 Interaction of fluid-solid interaction

Under post-processing, the solution for fluent can be found by examining various factors such as deformation, Von Mises equivalent stress, strain energy, and pressure. Piezoelectric patch undergoes periodic deformation when subjected to a fluctuating force, with the highest deformation equaling $7.0689*10^{-10}$ Figures 14 and 15, respectively, present the simulation results for the velocity contour, pressure contour, Von misses stress and deformation variables. Figure 16 depicts the corresponding stress on the patch; Figure 17 depicts the change in a patch's deformation at its various nodes. Figure 18 depicts the maximum deformation over six frequencies at various mode-shape frequencies. It can be seen from the simulated results that the maximal stress at the bottom of the piezo-patch and beam act is located towards the boundary of the fixation.
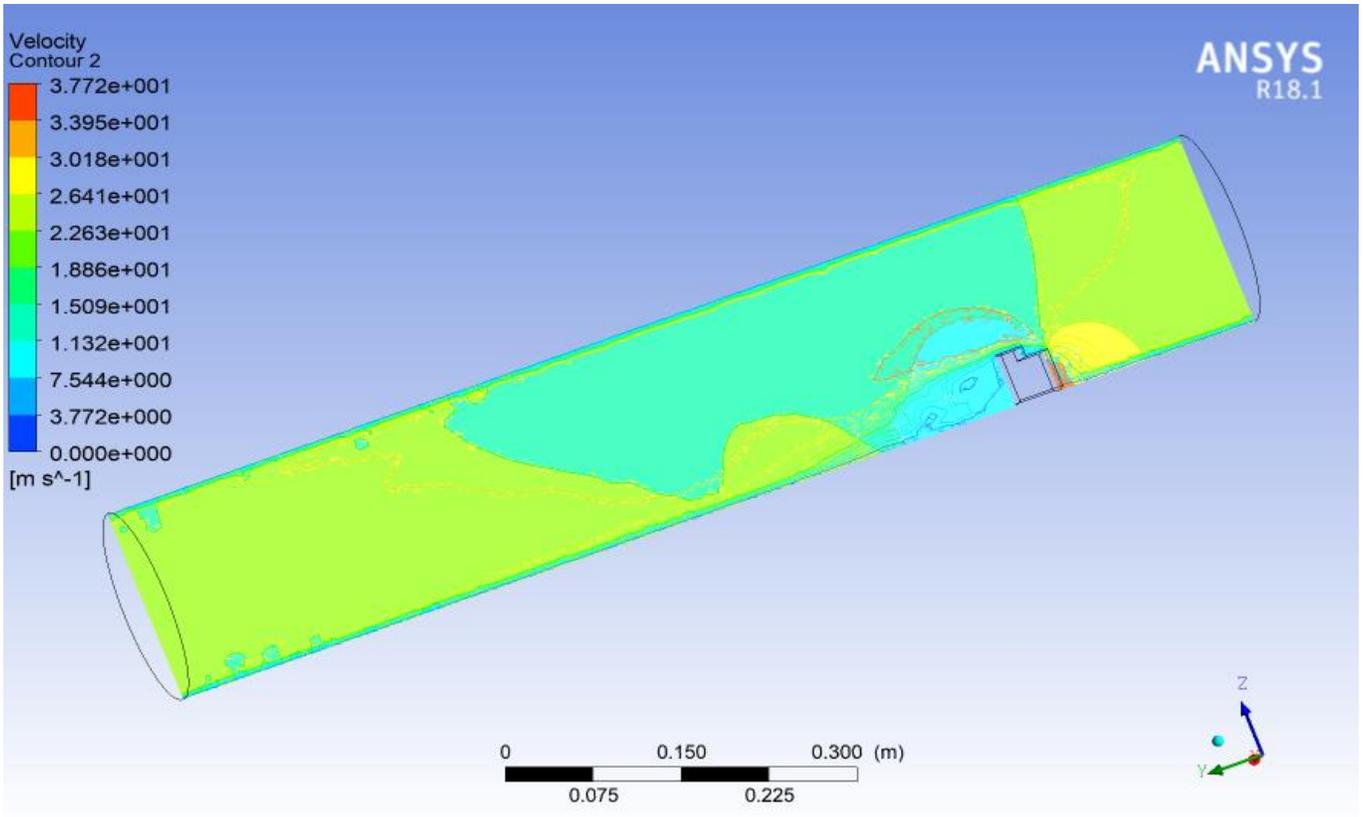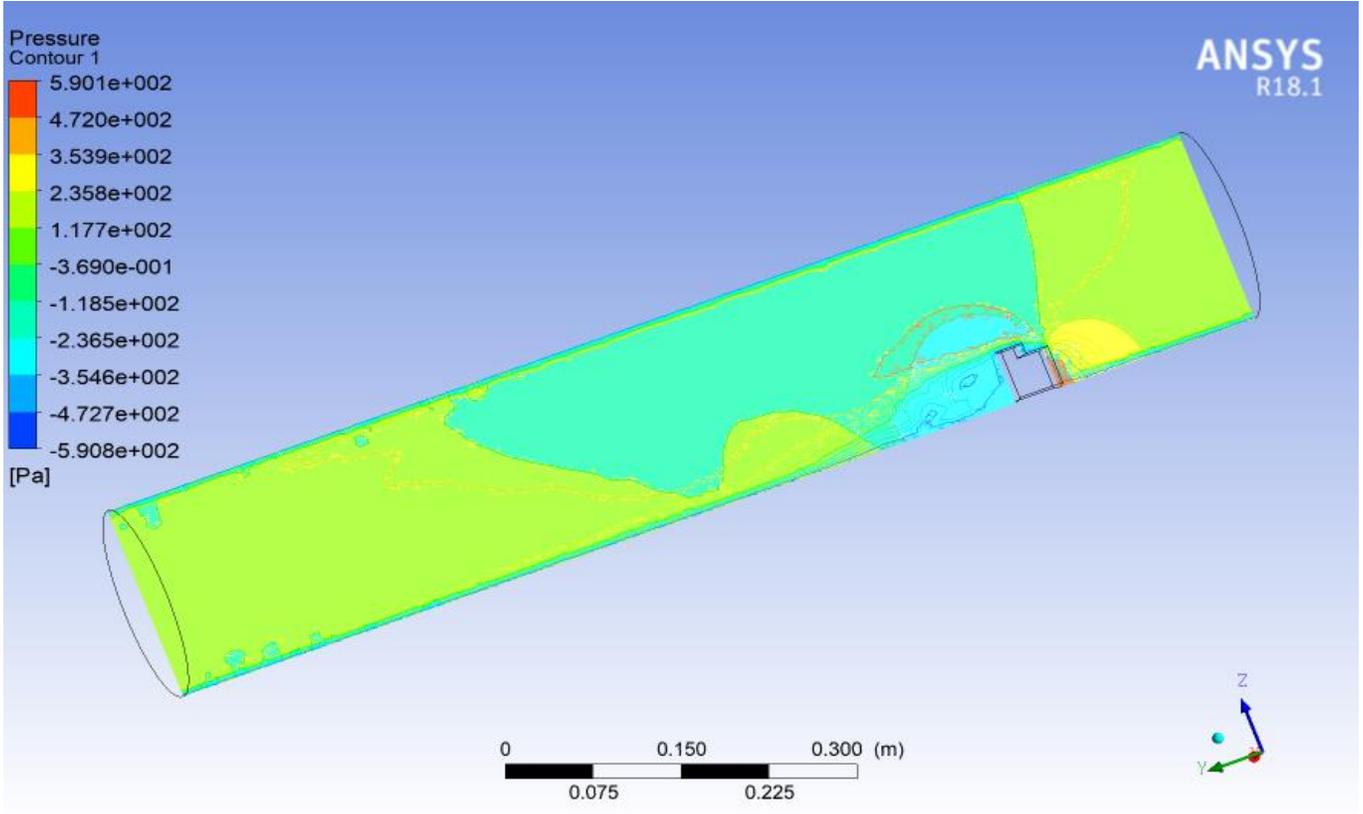
Fig. 12 Velocity contour
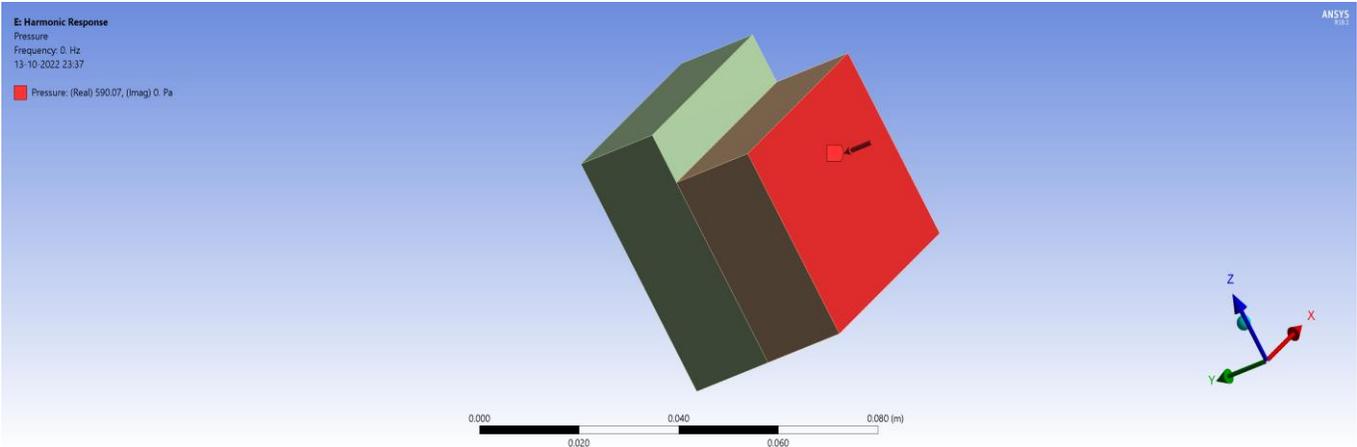

Fig. 13 Pressure contour

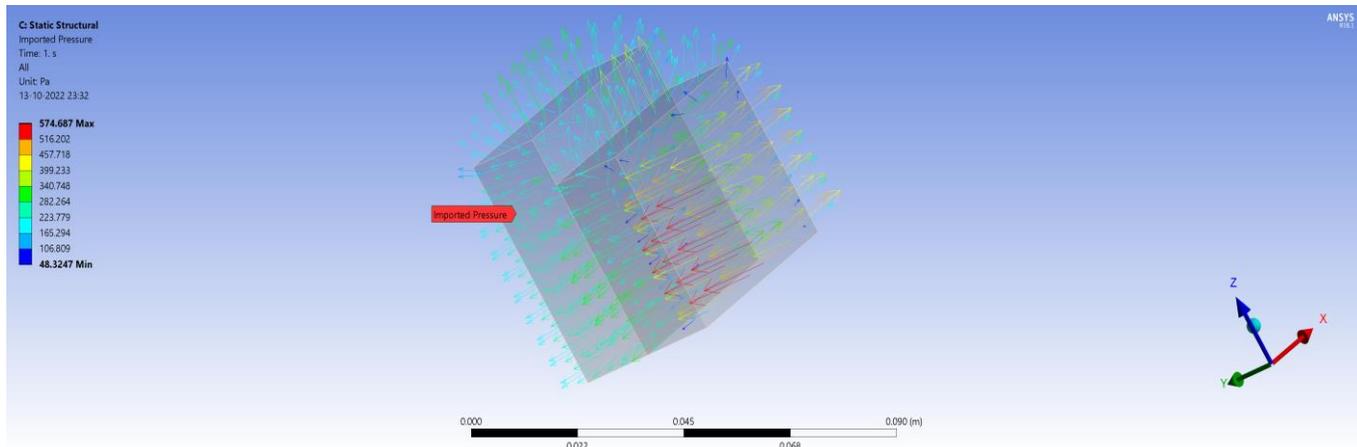**Fig. 14 Pressure exerted on the face of the piezoelectric patch**

Fig. 15 Imported pressure on the piezoelectric patch and beam arrangement

Von misses equivalent stress at piezoelectric during the course of the simulation; the stress fluctuates from 19.496 Pa to 4288.1 Pa.The stationary analysis of this research has been done. When the fluid passes through the circular cylinder structure with an average velocity of 30 m/s along the cross-section of the body. Before it gets to the other side, The distribution of Von-Mises equivalent stress along the circular cylinder is shown in fig. 16 as
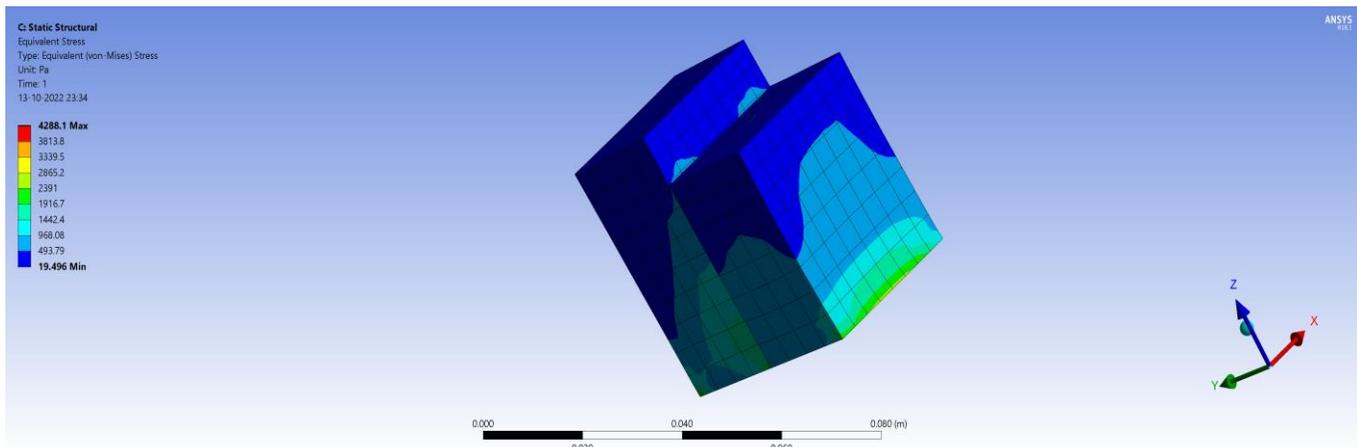

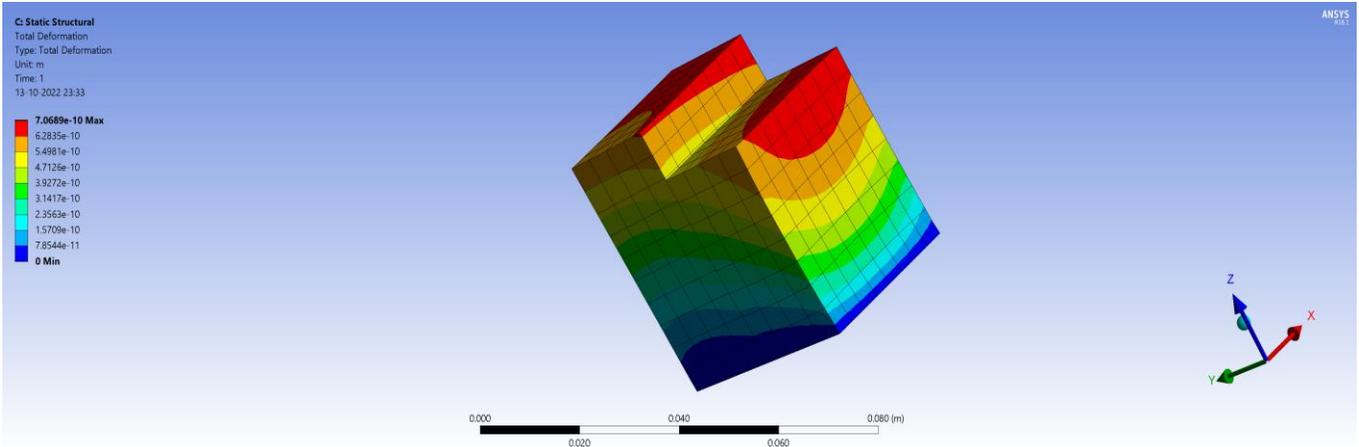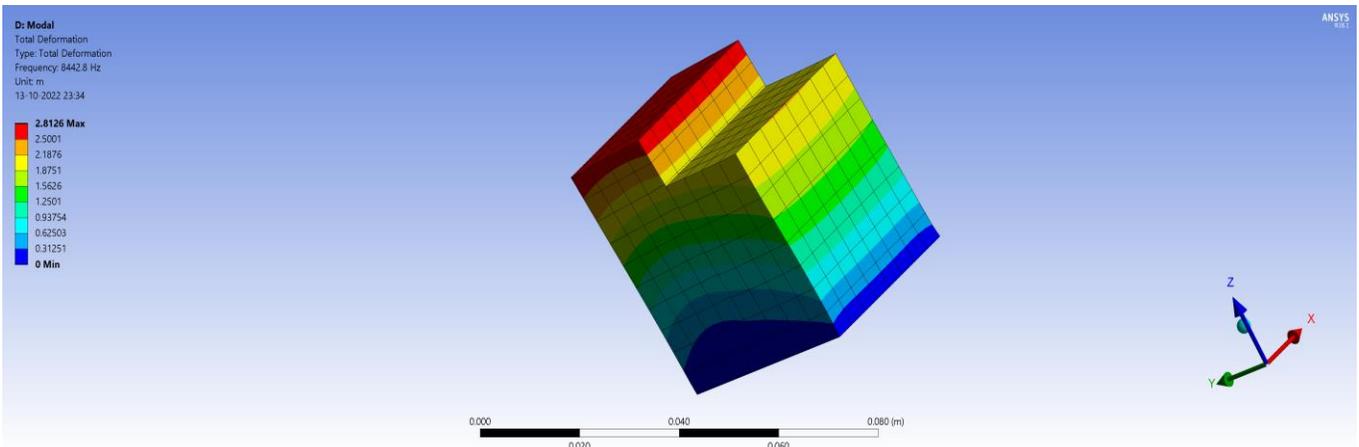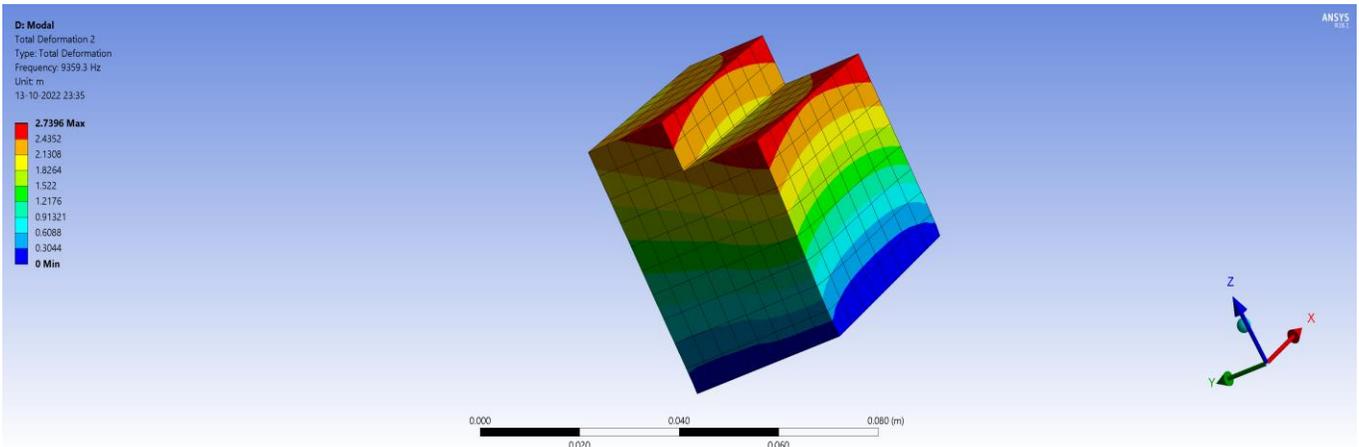**Fig. 16 Von-mises equivalent stress**

Fig. 17 Total deformation plot

(a)

(b)

(c)

(d)

(e)
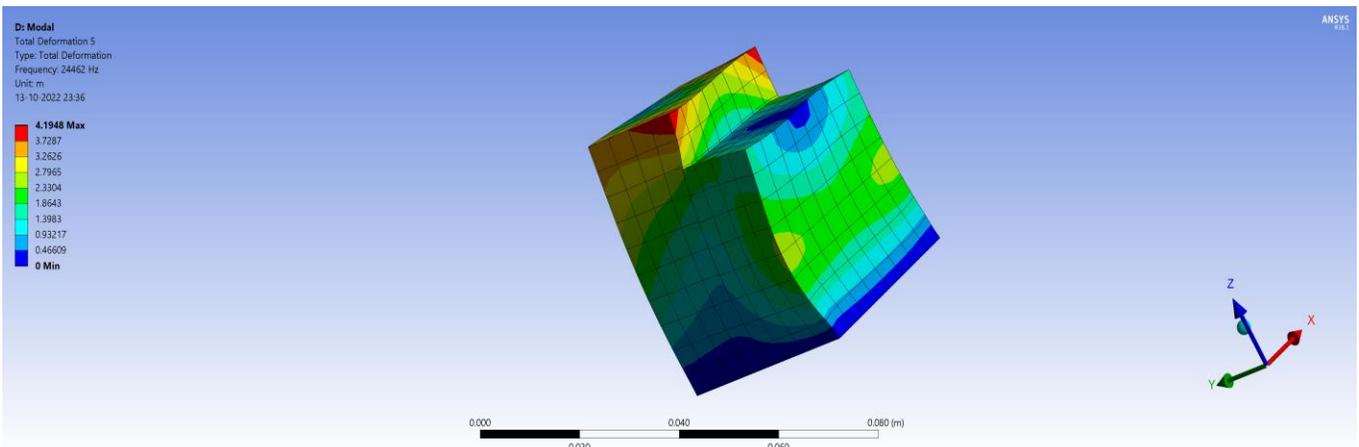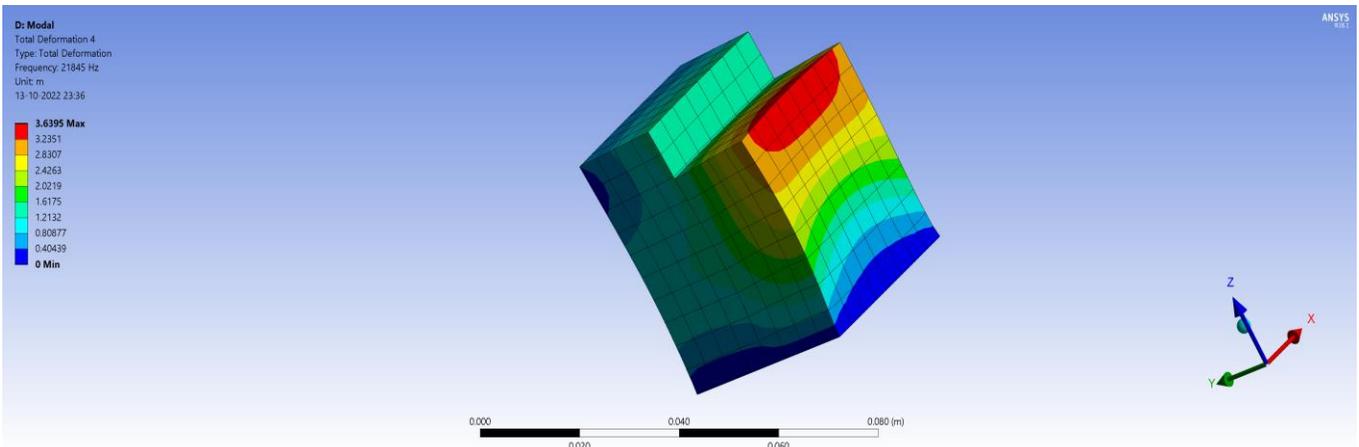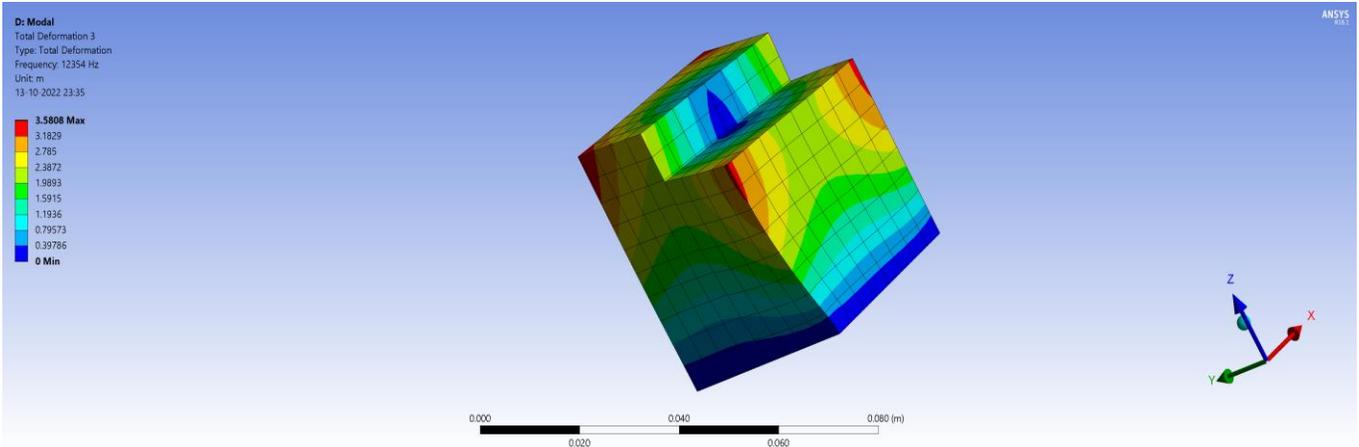
(f)
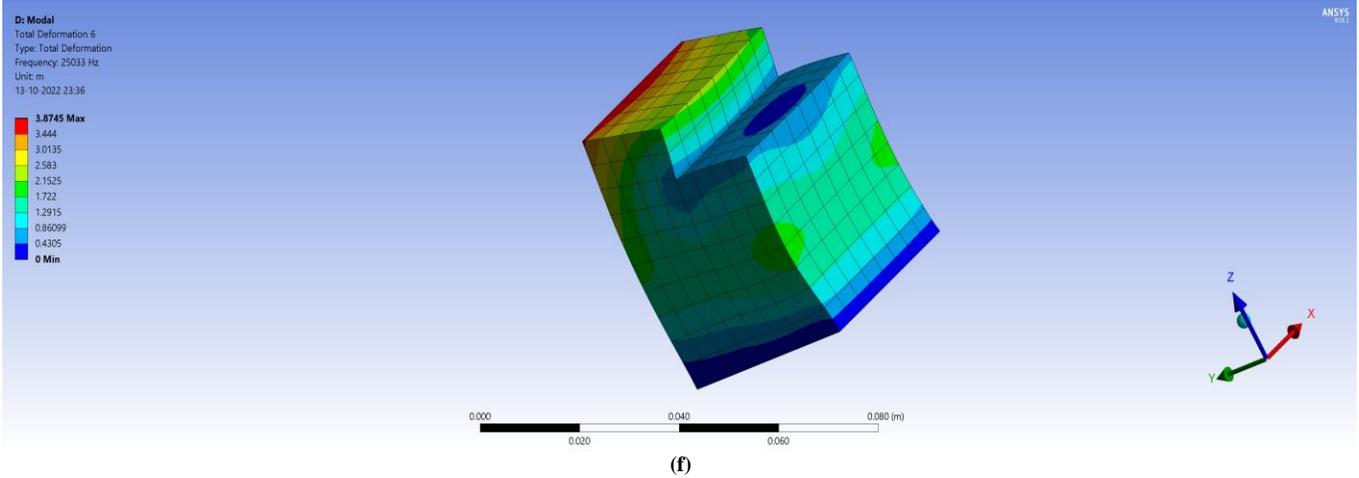**Fig. 18 Static structural deformation for above six mode shape frequencies (a-f)**

4. Governing Equations for Motion of Fluid with Constraints and Boundary Conditions

The following equations can be considered the principal equations of the flowing fluid, structure, and the interaction among them. The laminar model is only applicable to regions with average Reynolds numbers. Therefore, the velocities are seen in regions adjacent to the wall and caused by its impacts fall rapidly. In most cases, a wall function which relies on uniform velocity profiles is implemented to overcome this delima. In near-wall regions, it is not mandatory to use high mesh resolution. The stress caused by the tangential velocity vector in the cylindrical surface is equal to the normal stress.

4.1. Equation of Motion for Flowing of Fluid

Incompressible Navier-Stokes equations in laminar flow & continuity equations have been formulated and solved for the discretization of fluids.

$$\rho(u \bullet \nabla)u = \nabla \bullet [-pI + k] + F \quad (1)$$
$$\rho(\nabla \bullet u) = 0 \quad (2)$$
$$k = \mu(\nabla u + (\nabla u)^T) \quad (3)$$

$\rho \rightarrow$ Density of fluid, u$\rightarrow$ Velocity of fluid, $\mu \rightarrow$Dynamic Viscosity, $I \rightarrow$ Identity Tensor

4.2. Initial Values of Parameters

The initial value that has been assigned for the inlet velocity of the global coordinates system for the y-axis is 30 m/s, while for the rest of the axis, it is 0, as seen in table 2. The initial value of gauge pressure was assigned to 0 [Pa]. The relative cell zone is utilized as the coordinate system for the standard initialization of the solution.

Table 2. Initial Values of Assigned parameters

Parameters	Values
u_x	0
u_z	0
u_y	30
p_i	0

$u_x, u_z, u_y \rightarrow$ Initial velocity of the fluid along the x, z, and y-axis, respectively, $p_i \rightarrow$ Initial Gauge Pressure

4.3. Equations for Movement of Wall

In the case of the laminar layer's wall function of fluid-solid interaction zone with stationary wall movement in no-slip condition, the shear condition is given by the mathematical equation

$$u=0 \quad (4)$$

4.4. Inlet Flow Equations for Fluid

A normal component of the velocity of flowing fluid by using the nodal constraint nodal method for inlet flow is given by

$$u = -U_0 n \quad (5)$$

$$U_{ref} = U_0 \quad (6)$$

U_0 represents the mean velocity of flow via fluid input, Normal inflow velocity, U_0=30 under a specific laminar length scale and intensity, and the normal unit vector is denoted by n.

4.5. Outlet Flow Equation for fluid

Outlet pressure has been taken w.r.t the absolute reference frame, and the path of backflow pressure has been used as the normal to the boundary with the specification method. The exerted pressure of flowing water is given by equations

$$[-pI + k]n = -\hat{p}_0 n \quad (7)$$

$$\hat{p}_0 \leq p_0 \quad (8)$$

p_0= 0 with suppress backflow $\quad (9)$
κ is von karman constant

Where p_0 is the pressure at the outlet flow

4.6. Vibrational and Oscillational Motion of Structure

As the interaction of fluid and the circular cylinder has taken place, the phenomena of vortex flow vibrations came into effect with fluid-induced motion. While, for the case of steady-state flowing fluid, the relation of the cylinder with vortices has been analyzed in the form of a Reynolds number. The relation between Reynolds number (R_e), the diameter of the circular cylinder (D), kinematic viscosity(v), and stream velocity (U) is given by

$$R_e = \frac{UD}{v} \tag{10}$$

As the moving fluid approaches the cylinder, then the oscillating flow mechanism of the system generates the frequency of vortex shedding, which has been concisely explained by Strouhal number (S_t). The relation between Strouhal number (S_t) with streamflow velocity (U), the diameter of the right cylinder (D), and the frequency of vortex shedding (f_s) is given by

$$S_t = \frac{Df_s}{U} \tag{11}$$

5. Constitutive Equations of Piezoelectric

The constitutive equations used in the piezoelectric process have been given:

$$\delta = Ed + \frac{\sigma}{Y} \tag{12}$$

$$D_e = \sigma d + E\varepsilon \tag{13}$$

Where $\delta \rightarrow$ Mechanical strain, E$\rightarrow$ Electric field, d $\rightarrow$ Coefficient of piezoelectric strain, Y$\rightarrow$ Young's modulus, σ $\rightarrow$ Mechanical stress, $D_e \rightarrow$Electric displacement, ε $\rightarrow$Dielectric constant

6. Mathematical Modeling of Generation of Voltage by the Piezoelectric Materials with Fundamentals

For a uni-dimensional piezoelectric material, the electric field E, the electrical induction D, mechanical strain S, electric field compliance s, and stress T. The linear electrical behavior of the material,

$$D = \varepsilon E \tag{14}$$

Hooks Law for linear elastic material,

$$S = sT \tag{15}$$

When an external force has been exerted on piezo-smart materials, it results in an electric charge density D in an electric charge (Q)on the electrodes of area A as

$$Q = DA \tag{16}$$

The voltage obtained from this is

$$V = \frac{Q}{C} \tag{17}$$

The density of electric charge has been given by

$$D = dT \tag{18}$$

Where T=$d\frac{F}{A}$, C=$\frac{\varepsilon^T A}{t}$ and t is the thickness of the piezo-patch

$$\tag{19}$$

When a certain amount of force is applied to a piezoelectric material, the resulting voltage can find out by

$$V = \frac{Ftd}{A\varepsilon^T} \tag{20}$$

Where F$\rightarrow$ Force applied on piezo-patch, t$\rightarrow$ Piezoelectric material thickness, d$\rightarrow$ piezoelectric charge coefficient, $\varepsilon^T \rightarrow$ Dielectric permittivity
Area of the rectangular piezoelectric patch

$$(A) = L_{PZT}B_{PZT} \tag{21}$$

$$\text{Relative permittivity}(\varepsilon_r) = \frac{\varepsilon}{\varepsilon_0} \tag{22}$$

Where $\varepsilon_0 \rightarrow$ Vacuum Permittivity
The generation of voltage is given by

$$V = \frac{KFtd}{A\varepsilon_r \varepsilon_0} \tag{23}$$

Where K is the piezoelectric coupling factor

7. Mathematical Modeling of Interaction of Fluid with the Rectangular Piezoelectric Patch

As the rectangular piezoelectric patch has been placed in the fluid with density 'ρ', inertial coefficient (C_i)and drag coefficient (C_d) have come into play. The total inline force has been exerted by a fluid on the rectangular piezoelectric patch can be calculated mathematically with the help of the Morison equation as follows

$$F = \frac{1}{2}\rho DuC_d|u| + \frac{\pi D^2}{4}\rho C_i \frac{du}{dt} \tag{24}$$

Where
F$\rightarrow$ Exerted inline force in the direction of the fluidic wave,
ρ$\rightarrow$ fluid's density,
D$\rightarrow$ Rectangular Piezo-patch diameter,
u $\rightarrow$Flowing fluid velocity,
$C_d \rightarrow$ Drag's Coefficient,
$C_i \rightarrow$Inertial Coefficient,
$\frac{du}{dt} \rightarrow$ Acceleration of flowing fluid
Voltage,

$$V = \left[\frac{Ktd}{\varepsilon_r \varepsilon_0}\right]\frac{F}{A} = \left[\frac{Ktd}{\varepsilon_r \varepsilon_0}\right]\left[\frac{\frac{1}{2}\rho DuC_d|u| + \pi \frac{D^2}{4}\rho C_i \frac{du}{dt}}{L_{PZT}B_{PZT}}\right] \tag{25}$$

If R denotes the resistance produced by the piezoelectric patch having the distance L_c of conductor with the area of rectangular piezoelectric patch A, breadth of the patch B_{PZT}, specific resistance ρ such as

$$R = \frac{\rho}{A}L_c = \left[\frac{\rho}{L_{PZT}B_{PZT}}\right]L_C \tag{26}$$

If r denotes conductivity, q denotes resistivity, and R denotes the resistance of a rectangular piezo-patch with length L_{PZT} and area A, then the power produced by this voltage V as

$$P = \frac{V^2}{R} = \frac{\left[\left[\frac{Ktd}{\varepsilon_r \varepsilon_0}\right]\left[\frac{\frac{1}{2}\rho D u C_d |u| + \frac{\pi D^2}{4}\rho C_i \frac{du}{dt}}{L_{PZT} B_{PZT}}\right]\right]^2 L_{PZT} B_{PZT}}{\rho L_c}$$

(27)

Energy(E) generated by the piezoelectric patch is given by

$$E = \left[\frac{V^2}{R}\right]t = \frac{\left[\left[\frac{Ktd}{\varepsilon_r \varepsilon_0}\right]\left[\frac{1}{2}\rho D u C_d |u| + \frac{\pi D^2}{4}\rho C_i \frac{du}{dt}\right]\right]^2}{\rho L_c L_{PZT} B_{PZT}}t$$

(28)

So, in this way, a quite suitable relationship between flowing fluid and voltage, power, and energy generation by piezoelectric material has been obtained.

8. Results and Discussion

In the current study, experimental and analytical analysis has been integrated to look into the feasibility of generating micro-energy from flowing fluid-based induced vibration over rectangular piezo-patch PZT 5A patches with a beam mechanism system placed in a cylindrical bluff body. A renewable energy harvesting model simulation was constructed for the purpose of replicating the properties of a piezo patch in the wake of a cylindrical structure. This was done with the intention of providing additional vision into the operation of fluid-based energy harvesters. An investigation was conducted to determine the magnitudes and locations of the most significant stresses. During the simulations, the flow model of ANSYS software was utilized, and water was chosen as the fluid of interest. At the same time, structural steel was used as the solid component for the cylinder. Rectangular piezoelectric material employed was Lead Zirconate Titanate (PZT 5A) patches, and The beam has been assigned with the material structure steel annealed. The simulation duration was noticed as 5 seconds, and the time steps were 0.01 seconds, resulting in an approximate computation time of 41 seconds when using an Intel Core i5-5300U CPU processing at 2.30 GHz,16 G.B. of RAM, and a 64-bit operating system. For a certain diameter and length of the cylindrical bluff body and a set of dimensions of Lead Zirconate Titanate (PZT 5A), an analysis was carried out to determine the regions of peak stresses and electrical potential on the body. Figure 2 and figure 5 shows the geometry of the three-dimensional cylindrical body and the mesh in the fluid domain with structure, respectively. The displacement of the cylindrical body and the accompanying induced electrical potential at a certain velocity are the things that need to be determined for the purposes of this investigation. It has been observed that the beam-piezoelectric patch arrangement system vibrates as a result of the viscous and pressure forces of fluid strikes on the system with an average velocity of '30 m/s'.

Consequently, a distortion generates in the domain of the flowing fluid. The higher the flow velocity away from the bluff body, the more intense the color of the streamlines. Figure 16 shows the beam's Von-Mises-Stress distribution, and the largest Von-Mises stress is found at the bottom of the beam-piezo patch arrangement fixed with the stationary circular cylinder. In contrast, the least value is found at the upper portion of the piezo-beam arrangement of the circular cylindrical bluff body that is free to move. An accompanying color chart depicts the degree to which objects have moved. In the case of harmonic response, finding out the solution phase response and frequency response plot with respect to deformation can be generated by ANSYS simulation solution by selecting the vertex of a beam with the direction of deformation in y–axis, average spatial resolution.

The pressure output plot of the deformed structure w.r.t sweeping phase(•) for 300 Hz frequency in the duration of 720°can is depicted in fig 19. It can be seen from the phase response graph that as the value exerted increases with the sweeping phase, the output response has been decreases and vice versa. The frequency response amplitude plot with a frequency range of 0 to 1000 Hz and subinterval of 10 Hz each can be shown in fig. 20. As the frequency value increases, the response amplitude decreases rapidly, i.e. behaves inversely in the direction of deformation.

The voltage frequency plot can be seen in fig. 21 with amplitude voltage and frequency plot. From fig. 21, it has been noticed that the value of frequency rises, and the amplitude of the voltage also rises. Similarly, it was observed that the voltage that was produced by the laminar flowing water at the middle of the patch as a result of the deformation of the piezo material was 0.026 V. In order to confirm the novelty of the current model, simulation findings and mathematical modeling were compared for key output factors [28, 58]. Table 3 demonstrates that the output generated from the simulation correlates well with mathematical findings with a percentage error of 3.846.

Table 3. Evaluation of generated voltage

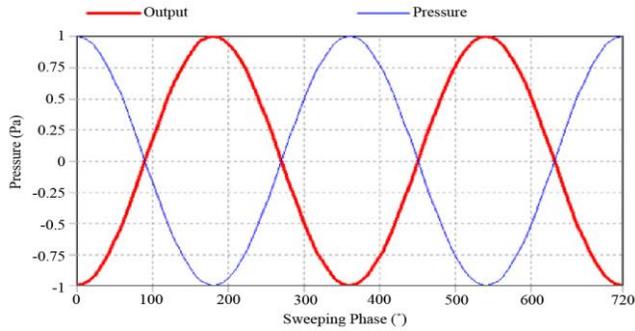| Sr. No.	Value of Factor	Simulation Result	Mathematical Modeling Result	Error Percentage
1.	Voltage output w.r.t exerted pressure	0.026V	0.025V	3.846

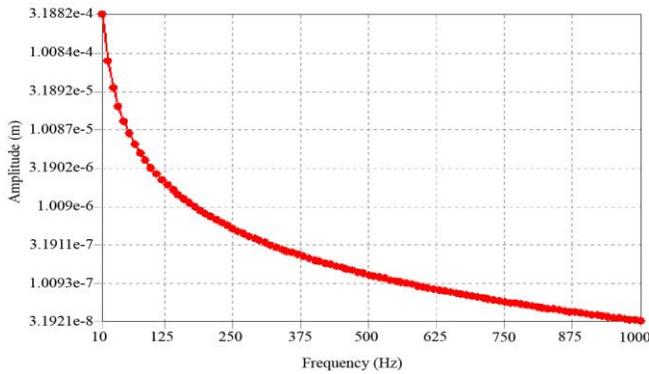**Fig. 19 Pressure output vs sweeping phase plot**

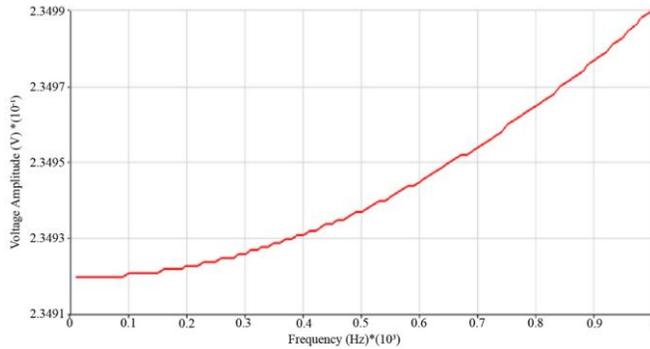**Fig. 20 Frequency response vs amplitude deformation plot**

Fig. 21 Voltage amplitude vs frequency plot

9. Conclusion

The proposed work has concluded that a part of the kinetic energy of a laminar, incompressible, and steady-flowing fluid can be changed into electrical energy by placing a beam and rectangular piezoelectric patch arrangement system attached within the circular cylindrical structure. This was accomplished by striking the fluid on a cylindrical structure with an average velocity of '30 m/s' at a separation of '202.698 mm' from the inlet of the circular cylinder. A laminar flow mathematical model has been used for the numerical computation of circular cylindrical structures. To simulate real-world conditions, ANSYS has been utilized for finite element analysis (FEA). Following this, a 3D simulation model was created to determine the voltage, electrical power, total deformation, Von Mises stress, strain, frequency response, phase response, and amplitude graphs. With an average fluid flow rate of 30 m/s, an electric voltage of amplitude of up to near 0.026 V across the piezoelectric domain has been observed. It has been noticed that findings obtained from the simulation efficiently validate the findings of mathematical modeling with an error percentage of 3.846. The assigned frequency directly influences the generation of voltage. The resulting generated voltage can be efficiently utilized for electrical appliances like bulbs, mobile charging, and various other micro-devices. Hence, it is an efficient source of voltage creation since it is quite simple to combine with other structures, eco-friendly, non-expensive, weightless, and requires much less setup space. Industrial wastes, domestic wastes, and canal and river water can be used as feasible sources of voltage generation. Turbulent flow also can be an interesting source of voltage generation at the micro level in the forthcoming future.

Acknowledgments

References

[1] S. O. Ganiyu, C. A. Martínez-Huitle, and M. A. Rodrigo, "Renewable Energies Driven Electrochemical Wastewater/Soil Decontamination Technologies: A Critical Review of Fundamental Concepts and Applications," *Applied Catalysis B: Environmental*, vol. 270, p. 118857, 2020. *Crossref*, https://doi.org/10.1016/j.apcatb.2020.118857

[2] B. K. Bose, "Global Warming: Energy, Environmental Pollution, and the Impact of Power Electronics," *IEEE Industrial Electronics Magazine*, vol. 4, no. 1, pp. 6-17, 2010. *Crossref*, https://doi.org/10.1109/MIE.2010.935860

[3] A. B. Rostami, and A. Mohammadmehdi, "Renewable Energy Harvesting by Vortex-Induced Motions: Review and Benchmarking of Technologies," *Renewable and Sustainable Energy Reviews*, vol. 70, pp. 193-214, 2017. *Crossref*, https://doi.org/10.1016/j.rser.2016.11.202

[4] M. Yadav et al., "Modeling and Optimization of Piezoelectric Energy Harvesting System under Dynamic Loading," *Advances in Fluid and Thermal Engineering*, pp. 339-353, 2021. *Crossref,* https://doi.org/10.1007/978-981-16-0159-0_30

[5] N. Kumar, and G. Singh, "A Novel Algorithm to Improve the Power Quality for the Smart Grid and Integration with the Optimization Framework," *International Journal of Engineering Trends and Technology*, vol. 69, no. 9, pp. 272-280, 2021. *Crossref*, https://doi.org/10.14445/22315381/IJETT-V69I9P233

[6] M. Yadav et al., "Experimental & Mathematical Modeling and Analysis of Piezoelectric Energy Harvesting with Dynamic Periodic Loading," *International Journal of Recent Technology and Engineering*, vol. 8, no. 3, pp. 6346-6350, 2019. *Crossref*, http://www.doi.org/10.35940/ijrte.C6107.098319

[7] S. Mishra et al., "Advances in Piezoelectric Polymer Composites for Energy Harvesting Applications: A Systematic Review," *Macromolecular Materials and Engineering*, vol. 304, no. 1, p. 1800463, 2019. *Crossref*, https://doi.org/10.1002/mame.201800463

[8] S. M. Khot et al., "Experimental Investigation of Performances of Different Optimal Controllers in Active Vibration Control of a Cantilever Beam," *ISSS Journal of Micro and Smart Systems*, vol. 8, no. 2, pp. 101-111, 2019. *Crossref*, https://rb.gy/nouhgn

[9] S. Abrol, and D. Chhabra, "Experimental Investigations of Piezoelectric Energy Harvesting with Turbulent Flow," *International Journal of Mechanical and Production Engineering Research & Development*, vol. 8, no.1, pp. 703-710, 2018. *Crossref*, http://dx.doi.org/10.24247/ijmperdfeb201877

[10] S. Meninger et al., "Vibration-to-Electric Energy Conversion," *Proceedings of the 1999 International Symposium on Low Power Electronics and Design*, pp. 48-53, 1999. *Crossref*, https://dl.acm.org/doi/pdf/10.1145/313817.313840

[11] X. Tang et al., "Energy Harvesting Technologies for Achieving Self-Powered Wireless Sensor Networks in Machine Condition Monitoring: A Review," *Sensors*, vol. 18, no. 12, p. 4113, 2018. *Crossref*, https://doi.org/10.3390/s18124113

[12] N. Kumar, and G. Singh, "A Study of ATC Losses, Tools, Techniques and Ongoing Applications in Smart Grid," *International Journal of Engineering Trends and Technology*, vol. 70, no. 3, pp. 140-150, 2022. *Crossref*, https://doi.org/10.14445/22315381/IJETT-V70I3P216

[13] A. Naqvi et al., "Energy Harvesting from Fluid Flow using Piezoelectric Materials: A Review," *Energies*, vol. 15, no. 19, p. 7424, 2022. *Crossref*, https://doi.org/10.3390/en15197424

[14] A. Q. Malik, "Renewables for Fiji–Path for Green Power Generation," *Renewable and Sustainable Energy Reviews,* vol. 149, p. 111374, 2021. *Crossref*, https://doi.org/10.1016/j.rser.2021.111374

[15] M. Hafizh et al., "A Hybrid Piezoelectric–Electromagnetic Nonlinear Vibration Energy Harvester Excited by Fluid Flow," *Mechanical Reports,* vol. 349, no. 1, pp. 65-81, 2021. *Crossref*, https://doi.org/10.5802/crmeca.74

[16] M. Parween, A. L. Ramanathan, and N. J. Raju, "Waste Water Management and Water Quality of River Yamuna in the Megacity of Delhi," *International Journal of Environmental Science and Technology,* vol. 14, no. 10, pp. 2109-2124, 2017. *Crossref*, https://link.springer.com/article/10.1007/s13762-017-1280-8

[17] Hafez Fouad, "A Highly Efficient 0.18um CMOS Rectifier For Vibrational Energy Harvesting System in Embedded Electronics Design," *SSRG International Journal of Electrical and Electronics Engineering*, vol. 7, no. 8, pp. 4-10, 2020. *Crossref*, https://doi.org/10.14445/23488379/IJEEE-V7I8P102

[18] S. Suhag, and D. Chhabra, "Design of a Closed Channel Fluid Flow System for Piezoelectric Energy Harvesting," *International Research Journal of Engineering and Technology*, vol. 5, no. 4, pp. 1960-1963, 2018.

[19] K. C. Mishra, "A Review on Supply of Power to Nanorobots Used in Nanomedicine," *International Journal of Advances in Engineering & Technology,* vol. 4, no. 2, p. 564, 2012.

[20] J. Bundschuh et al., "State-of-the-Art of Renewable Energy Sources Used in Water Desalination: Present and Future Prospects," *Desalination*, vol. 508, p. 115035, 2021.*Crossref*, https://doi.org/10.1016/j.desal.2021.115035

[21] M. Hidemi et al., "Harvesting Flow-Induced Vibration Using a Highly Flexible Piezoelectric Energy Device," *Applied Ocean Research,* vol. 68, pp. 39-52, 2017. *Crossref*, https://doi.org/10.1016/j.apor.2017.08.004

[22] L. Zhenyu et al., "Towards Sustainability in Water-Energy Nexus: Ocean Energy for Seawater Desalination," *Renewable and Sustainable Energy Reviews,* vol. 82, pp. 3833-3847, 2018. *Crossref*, https://doi.org/10.1016/j.rser.2017.10.087

[23] M. Safaei, H. A. Sodano, and S. R. Anton, "A Review of Energy Harvesting Using Piezoelectric Materials: State-of-the-Art A Decade Later (2008–2018)," *Smart Materials and Structures,* vol. 28, no. 11, p. 113001, 2019. *Crossref*, https://doi.org/10.1088/1361-665X/ab36e4

[24] Hafez Fouad, Hesham Kamel, and Adel Youssef, "Voltage-Booster for CMOS Wide-Band High-Precision Rectifier of Energy Harvesting for Implantable Medical Devices in Internet of Bodies (IOB) Telemedicine Embedded System," *SSRG International Journal of Electrical and Electronics Engineering*, vol. 9, no. 4, pp. 19-30, 2022. *Crossref*, https://doi.org/10.14445/23488379/IJEEE-V9I4P103

[25] D. Yadav et al., "Modeling and Simulation of an Open Channel PEHF System for Efficient PVDF Energy Harvesting," *Mechanics of Advanced Materials and Structures,* vol. 28, no. 8, pp.812-826, 2021. *Crossref*, https://doi.org/10.1080/15376494.2019.1601307

[26] W. Sun et al., "Energy Harvesting From Water Flow in Open Channel with Macro Fiber Composite," *AIP Advances,* vol. 8, no. 9, p. 095107, 2018. *Crossref*, https://doi.org/10.1063/1.5035383

[27] X. Shan et al., "Energy-Harvesting Performances of Two Tandem Piezoelectric Energy Harvesters with Cylinders in Water," *Applied Sciences,* vol. 6, no. 8, p. 230, 2016. *Crossref*, https://doi.org/10.3390/app6080230

[28] R. Song et al., "Modeling, Validation, and Performance of Two Tandem Cylinder Piezoelectric Energy Harvesters in Water Flow," *Micromachines*, vol. 12, no. 8, p. 872, 2021. *Crossref*, https://doi.org/10.3390/mi12080872

[29] C. Wei, and Xingjian Jing, "A Comprehensive Review on Vibration Energy Harvesting: Modelling and Realization," *Renewable and Sustainable Energy Reviews,* vol. 74, pp.1-18, 2017. *Crossref,* https://doi.org/10.1016/j.rser.2017.01.073

[30] N. Kumar, and G. Singh, "Comparative Study of Performance about the Integrated Power Quality and Optimized Framework for Smart Grid," *Journal of Technology Innovations and Energy*, vol. 1, no. 3, pp. 33-39, 2022. *Crossref,* https://doi.org/10.56556/jtie.v1i3.267

[31] Z. Yang, A. Erturk, and J. Zu, "On the Efficiency of Piezoelectric Energy Harvesters," *Extreme Mechanics Letters*, vol. 15, pp. 26-37, 2017. *Crossref,* https://doi.org/10.1016/j.eml.2017.05.002

[32] A. Jbaily, and R. W. Yeung, "Piezoelectric Devices for Ocean Energy: A Brief Survey," *Journal of Ocean Engineering and Marine Energy*, vol. 1, no. 1, pp. 101-118, 2015. *Crossref,* https://link.springer.com/article/10.1007/s40722-014-0008-9

[33] M. Subramani et al., "Efficient Energy Conservation from Hybrid Vehicle," SSRG International Journal of Electrical and Electronics Engineering, vol. 9, no. 5, pp. 1-8, 2022. *Crossref,* https://doi.org/10.14445/23488379/IJEEE-V9I5P101

[34] H. J. Cheng, "Energy Harvesting from a Vortex Ring Using Highly Deformable Smart Materials," *University of Waterloo*, 2016. *Crossref,* http://hdl.handle.net/10012/10101

[35] S. M. Khot, and N. P. Yelve, "Modeling and Response Analysis of Dynamic Systems by using ANSYS© and MATLAB©," *Journal of Vibration and Control*, vol. 17, no. 6, pp. 953-958, 2011. *Crossref,* https://doi.org/10.1177/1077546310377913

[36] M. Zhou et al., "Piezoelectric Wind Energy Harvesting Device Based on the Inverted Cantilever Beam with Leaf-Inspired Extensions," *AIP Advances*, vol. 9, no. 3, p. 035213, 2019. *Crossref,* https://doi.org/10.1063/1.5082811

[37] S. M. Khot et al., "Active Vibration Control of Cantilever Beam by using PID Based Output Feedback Controller," *Journal of Vibration and Control*, vol. 18, no. 3, pp. 366-372, 2012. *Crossref,* https://doi.org/10.1177/1077546311406307

[38] E. Alaei, H. Afrasiab, and M. Dardel, "Analytical and Numerical Fluid–Structure Interaction Study of a Microscale Piezoelectric Wind Energy Harvester," *Wind Energy*, vol. 23, no. 6, pp. 1444-1460, 2020. *Crossref,* https://doi.org/10.1002/we.2502

[39] S. M. Khot, N. P. Yelve, and R. Iyer, "Extraction of System Model from Finite Element Model and Simulation Study of Active Vibration Control," *Advances in Vibration Engineering*, vol. 11, no. 3, pp. 259-280, 2012. *Crossref,* https://rb.gy/yujfpx

[40] M. Yadav et al., "State of Art of Different Kinds of Fluid Flow Interactions with Piezo for Energy Harvesting Considering Experimental, Simulations and Mathematical Modeling," *Journal of Mathematical and Computational Science*, vol. 11, no. 6, pp. 8258-8287, 2021. *Crossref,* http://scik.org/index.php/jmcs/article/view/6772

[41] M. Yadav, "A Review on Piezoelectric Energy Harvesting Systems Based on Different Mechanical Structures," *International Journal of Enhanced Research Science Technology Engeering,* vol. 9, no. 1, pp. 1-7, 2020.*Crossref,* https://rb.gy/w8mdzx

[42] M. Yadav, and D. Yadav, "Micro Energy Generation in Different Kinds of Water Flows on Lead Zirconium Titanite/PVDF," *International Journal of R&D in Engineering, Science and Management*, vol. 9, no. 5, pp. 1-8, 2019. *Crossref,* https://doi.org/10.13140/RG.2.2.22377.85606

[43] N. Kumar, and G. Singh, "Energy Efficient Load Optimization Techniques for Smart Grid with Futuristic Ideas," *International Journal of Engineering and Advanced Technology*, vol. 9, no. 1, pp. 4327-4331, 2019. *Crossref,* https://rb.gy/qj8lrv

[44] D. Chhabra, and A. Kumar, "Study of PEH Configurations & Circuitary and Techniques for Improving PEH Efficiency," *International Journal for Scientific Research & Development,* vol. 4, no. 3, 2016.

[45] N. Yadav, and D. Chhabra, "Design and Analysis of Closed Flow System with Varying Various Parameters of Hydrodynamics for PEH," *Journal of Control & Instrumentation*, vol. 8, no. 3, pp. 30-37, 2017. *Crossref,* https://doi.org/10.37591/joci.v8i3.253

[46] S. Priya et al., "A Review on Piezoelectric Energy Harvesting: Materials, Methods, and Circuits," *Energy Harvesting and Systems,* vol. 4, no. 1, pp. 3-39, 2017. *Crossref,* https://doi.org/10.1515/ehs-2016-0028

[47] D. Chhabra, G. Bhushan, and P. Chandna, "Multilevel Optimization for the Placement of Piezo-Actuators on Plate Structures for Active Vibration Control Using Modified Heuristic Genetic Algorithm," *Industrial and Commercial Applications of Smart Structures Technologies*, vol. 9059, pp. 152-161, 2014. *Crossref,* https://doi.org/10.1117/12.2044913

[48] D. Chhabra, "Optimal Placement of Piezoelectric Actuators on Plate Structures for Active Vibration Control via Modified Control Matrix and Singular Value Decomposition Approach using Modified Heuristic Genetic Algorithm," *Mechanics of Advanced Materials and Structures,* vol. 23, pp. 458-463, 2014. *Crossref,* https://doi.org/10.1080/15376494.2014.949932

[49] S. Kumar, and D. Chhabra, "Optimal Placement of Piezoelectric Actuators on Plate Structures for Active Vibration Control using Genetic Algorithm," *Active and Passive Smart Structures and Integrated Systems*, vol. 9057, pp. 647-659, 2014. *Crossref,* https://doi.org/10.1117/12.2044904

[50] N. Yadav, and R. Kumar, "Study on Piezoelectric Ceramic under Different Pressurization Conditions and Circuitry," *Journal of Electroceramics*, vol. 47, pp. 79-88, 2021. *Crossref,* https://link.springer.com/article/10.1007/s10832-021-00268-1

[51] N. Yadav, and R. Kumar, "Energy Harvesting from Low-Frequency Sinusoidal Vibrations using Diaphragm Type Piezoelectric Element," *Indian Journal of Engineering & Materials Sciences,* vol. 28, no. 3, pp. 265-270, 2021. *Crossref,* https://rb.gy/xfh4eu

[52] N. Yadav, and R. Kumar, "Harvesting Electric Energy from Waste Vibrations of an Electric Motor using the Piezoelectric Principle," *Recent Advances in Manufacturing, Automation, Design and Energy Technologies*, pp. 955-964, 2022. *Crossref,* http://dx.doi.org/10.1007/978-981-16-4222-7_104

[53] J. Yadav et al., "Green Energy Generation Through PEHF–A Blueprint of Alternate Energy Harvesting," *International journal of green energy*, vol. 16, no. 3, pp. 242-255, 2019. *Crossref*, https://doi.org/10.1080/15435075.2018.1562930

[54] S. K. Jha, S. Nallusamy, and S. A. Diwakar, "Future Energy Scenario in India-An Essential Overview," *Pollution Research,* vol. 35, no. 3, pp. 595-599, 2016. *Crossref*, https://rb.gy/qsyqi5

[55] A. Kumar, A. Kumar, and D. Chhabra, "Analysis of Smart Structures with Different Shapes of Piezoelectric Actuator," *International Journal of R&D in Engineering, Science and Management*, vol. 1, no. 2, pp.60-71, 2014. *Crossref*, https://rb.gy/qfkfea

[56] Samanta, S. Kumar, and C. K. Chanda, "Analysis of Voltage Stability in Smart Grid System Due to Demand Load Variation," *Advanced Energy and Control Systems*, pp. 123-136, 2022. *Crossref*, https://link.springer.com/chapter/10.1007/978-981-16-7274-3_10

[57] N. N. Sadullaev et al., "Increasing Energy Efficiency and Reliability of Electric Supply of Low Power Consumers," *SSRG International Journal of Engineering Trends and Technology*, vol. 68, no. 12, pp. 43-47, 2020. *Crossref*, https://ijettjournal.org/archive/ijett-v68i12p208

[58] M. Yadav et al., "Piezo-Beam Structure in a Pipe with Turbulent Flow as Energy Harvester: Mathematical Modeling and Simulation," *Journal of The Institution of Engineers (India): Series D*, vol. 103, no.2, 2022. *Crossref,* https://doi.org/10.1007/s40033-022-00440-z

[59] A. Kumar, and D. Chhabra, "Fundamentals of Piezoelectric Energy Harvesting," *International Journal for Scientific Research & Development*, vol. 4, no. 5, pp. 1168-1171, 2016. *Crossref*, https://www.ijsrd.com/articles/IJSRDV4I50751.pdf

[60] A. Kumar et al., "Design and Optimal Placement of PVDF Patches over a Shoe Transducer for Efficient Energy Harvesting," *Design Engineering*, vol. 1, no. 1, pp.08-22, 2020. *Crossref*, https://rb.gy/shgczw

[61] M. Muthusamy, and M. F. Jaafar, "Review of Wide-Frequency Bandwidth Piezoelectric Vibration Energy Harvester," *International Journal of Engineering Trends and Technology*, vol. 66, no. 3, 2018.
Crossref, https://ijettjournal.org/assets/year/2018/volume-66/IJETT-V66P228.pdf

[62] K. D. Aparna et al., "Design of Three Layer U-Shaped MEMS Piezoresistive Cantilever Using COMSOL Multiphysics," *International Journal of Engineering Trends and Technology*, vol. 67, no. 9, 2019.
Crossref, https://ijettjournal.org/assets/Volume-67/Issue-9/IJETT-V67I9P206.pdf

[63] R. Singh, N. S. Gill, and P. Gulia, "A Comparative Performance Analysis of Modeling and Simulation Tools for Smart Grid," *International Journal of Engineering Trends and Technology*, vol.70, no. 4, pp. 332-342, 2022.
Crossref, https://doi.org/10.14445/22315381/IJETT-V70I4P229

[64] C. V. Ochiegbu, S. Gyamfi, and E. Ofosu, "Modeling, Simulation and Design of Hydro-Solar Isolated Micro-grid without a Battery Storage System: A Case Study for Aba Business Cluster, Nigeria," *International Journal of Engineering Trends and Technology*, vol. 70, no. 2, pp.125-136, 2022. *Crossref*, https://ijettjournal.org/archive/ijett-v70i2p215

[65] N. Rai, H. L. Suresh, and V. S. Nagaraja, "Design, Modelling, and Simulation analysis of a Single Axis MEMS-based Capacitive Accelerometer," *International Journal of Engineering Trends and Technology*, vol. 69, no. 10, pp. 82-88, 2021.
Crossref, https://ijettjournal.org/archive/ijett-v69i10p211

[66] S. Panda et al., "Piezoelectric Energy Harvesting Systems for Biomedical Applications," *Nano Energy,* p. 107514, 2022.
Crossref, https://doi.org/10.1016/j.nanoen.2022.107514

[67] D. Yadav, and R. Sehrawat, "Green Energy Generation using Single and Double Parallel Circuit Configuration of PZT Piezoelectric Patch by Application of Hydro Dynamism," *International Journal of R&D in Engineering, Science and Management*, vol. 9, no. 2, pp. 25-38, 2019. *Crossref*, https://rb.gy/alrr3g

[68] M. Pasty, and P. M. Shirage, "Insights and Perspectives on Graphene-PVDF Based Nanocomposite Materials for Harvesting Mechanical Energy," *Journal of Alloys and Compounds*, vol. 904, p. 164060, 2022.
Crossref, https://doi.org/10.1016/j.jallcom.2022.164060